Analysis of Substrate Integrated Slab Waveguides (SISW) by the BI-RME Method

M. Bozzi[1], D. Deslandes[2], P. Arcioni[1], L. Perregrini[1], K. Wu[2], and G. Conciauro[1]

[1] Department of Electronics, University of Pavia, Pavia, Italy
[2] Poly-Grames Research Center, École Polytechnique de Montréal, Montréal, Canada

e-mail: bozzi@ele.unipv.it, deslad@grmes.polymtl.ca, arcioni@ele.unipv.it, perregrini@ele.unipv.it, wuke@grmes.polymtl.ca, conciauro@ele.unipv.it

Abstract— **This paper presents a novel method for the analysis of Substrate Integrated Slab Waveguides (SISWs), recently proposed as wideband integrated transmission lines. This method applies to the analysis of H–plane waveguides, filled with a dielectric medium perforated with air holes. The analysis is based on the segmentation technique combined with the BI-RME method, which permit to determine the generalized admittance matrix of the circuit and, finally, the dispersion diagram of the SISW. Some numerical and experimental results are reported.**

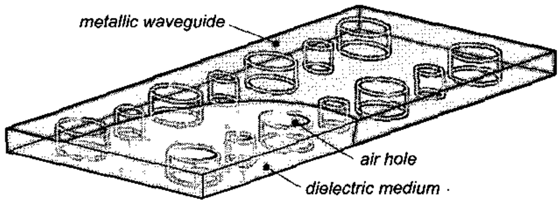

Fig. 1. Schematic of a Substrate Integrated Slab Waveguide.

I. Introduction

Substrate Integrated Slab Waveguides (SISWs) have been recently investigated [1] as wide–band transmission lines for the microwave and the millimeter wave range. SISWs consist of a rectangular waveguide filled with a dielectric medium, periodically perforated with air holes (Fig. 1).

The operation principle of SISWs is similar to the one of slab waveguides [2]: the electric field of the fundamental mode is mainly concentrated in the central portion of the waveguide, and therefore its cutoff frequency is strongly affected by the presence of the dielectric. Conversely, the electric field of the second mode is more concentrated in the side portions, where there is a lower equivalent dielectric permittivity. As a consequence, the bandwidth of the fundamental mode is significantly wider than in standard waveguides (twice as large, see [1]).

SISWs are easy to fabricate, compact, and cost effective. SISW technology may represent an interesting solution for many components (like frequency multipliers, directional couplers, power dividers) where wide bands are required.

In this work, we developed a novel method for the analysis of SISWs, based on the segmentation technique and the BI–RME method. The structure is segmented in a number of subcircuits, consisting of either the dielectric–filled portion or air holes. Each subcircuit is characterized separately by its Generalized Admittance Matrix (GAM). All GAMs are then recombined in order to determine the GAM of the whole structure. Once the GAM of the SISW is known, the dispersion diagram of the first modes can be calculated.

This paper describes the application of the BI–RME method and the technique for determining the dispersion diagram of SISW modes, and reports some numerical and experimental results.

This work was partially supported by the Quebec–Italy scientific and technological cooperation program 2000/02 and by the Italian Ministry of University and Scientific Research under F.I.R.B. program.

II. Analysis by the BI–RME Method

We consider an H–plane waveguide circuit filled with a dielectric medium, perforated with N air holes (Fig. 1). In principle, the method presented here applies to any planar circuit, and the cross–section of the holes can be arbitrary, even if only straight waveguide sections and circular holes have been used in this work. We assume that the tangential field at the ports of the waveguide (S_1 and S_2) is due to the combination of a number of TE_{p0} modes ($p = 1, \ldots, P$): therefore, the field inside the structure is z-independent, and the problem is two–dimensional. The aim of the analysis is the calculation of the GAM, which relates modal currents and voltages at ports S_1 and S_2.

A. Calculation of the Y-matrix

The analysis is based on the segmentation technique. The inhomogeneous H–plane waveguide (Fig. 2*a*) is divided into $N+1$ homogeneous subcircuits, one filled with dielectric (Fig. 2*b*), and N filled with air (Fig. 2*c*). Each subcircuit is analyzed separately, and characterized by its GAM.

In particular, when calculating the GAM of the dielectric–filled subcircuit, we must consider, besides the terminal waveguides ("external ports") S_1 and S_2, additional "connected ports" S_i $(i=3,N+2)$, corresponding to the interfaces between the dielectric–filled part and the air–filled holes (see Fig. 2*b*). On the external ports, the transverse electric and magnetic fields are expressed in the form

$$\vec{E}_i = \sum_{p=1}^{P_i} V_i^{(p)}\, \vec{e}_i^{(p)} \qquad (i=1,2) \tag{1}$$

$$\vec{H}_i = \sum_{p=1}^{P_i} I_i^{(p)}\, \vec{h}_i^{(p)} \qquad (i=1,2) \tag{2}$$

where $\vec{e}_i^{(p)}$ and $\vec{h}_i^{(p)}$ are the electric and magnetic modal vectors, respectively, of the TE_{p0} modes of the i–th port, and $V_i^{(p)}$ and $I_i^{(p)}$ are the corresponding modal voltages and currents; finally, P_i is the number of modes considered on port S_i $(i=1,2)$. On the connected ports, the transverse electric and magnetic fields are expressed in the form

$$\vec{E}_i = \sum_{p=1}^{P_i} V_i^{(p)}\, f_i^{(p)}\, \vec{u}_z \qquad (i=3,N+2) \tag{3}$$

$$\vec{H}_i = \sum_{p=1}^{P_i} I_i^{(p)}\, f_i^{(p)}\, \vec{n}\times\vec{u}_z \qquad (i=3,N+2) \tag{4}$$

where $f_i^{(p)}$ are z-independent scalar functions defined on S_i (sinusoidal functions in our implementation), $V_i^{(p)}$ and $I_i^{(p)}$ are the corresponding "voltages" and "currents", P_i is the number of functions considered on port S_i $(i=3,N+2)$, $\vec{n}$ is the inward normal on the inner boundary, and $\vec{u}_z$ is the unit vector in the z direction. As a consequence, the GAM of the dielectric–filled subcircuit relates currents $I_i^{(p)}$ to voltages $V_i^{(p)}$, corresponding to both external ports (defined on S_1 and S_2) and connected ports (defined on S_i, with $i=3,N+2$).

Since the dielectric–filled subcircuit is homogeneous, the Boundary Integral–Resonant Mode Expansion (BI–RME) method [3] can be used for the calculation of the GAM in the form of a pole–expansion in the frequency domain [4], [5]

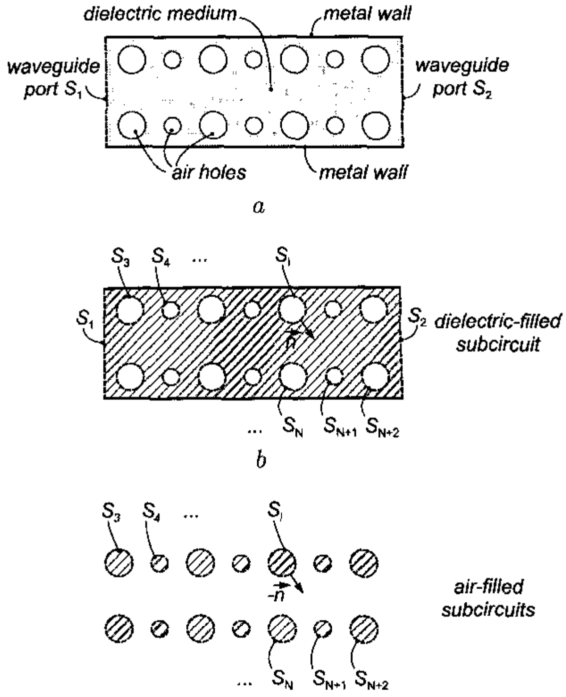

Fig. 2. Segmentation of the SISW component: (*a*) cross–section of the SISW; (*b*) cross–section of the dielectric–filled subcircuit; (*c*) cross–section of the air–filled subcircuits.

$$\mathbf{Y}(\omega) = \frac{\mathbf{A}}{j\omega} + j\omega\mathbf{B} + j\omega^3 \sum_{m=1}^{M} \frac{\mathbf{c}^{(m)}\mathbf{c}_{\mathrm{T}}^{(m)}}{\omega_m^2-\omega^2} \tag{5}$$

In (5), matrices $\mathbf{A}$, $\mathbf{B}$ are real and frequency independent, and are related to the quasi–static behavior of the admittance parameters. Moreover, ω_m represent the poles of the GAM, and are the resonant frequencies of the first resonating modes of the cavity obtained by short–circuiting all the ports, both external and connected. Finally, vectors $\mathbf{c}^{(m)}$ are real and independent of the frequency, and are related to the projection of the modal vector of the cavity on the port functions. As discussed in [3], to obtain a good accuracy in a frequency band from 0 to ω_{max}, it is sufficient to include in the pole expansion (5) only the M poles up to a frequency two or three times ω_{max}. All these quantities can be efficiently calculated by using the algorithm described in [4], [5], which was extended to take into account the presence of the connected ports.

In the case of the air holes (Fig. 2*c*), only connected ports are considered, and the expression of the fields on the ports are given by (3)–(4). Also in this case, the circuit is homogeneous, and the GAM can be expressed in the form of the pole expansion (5).

Once the GAMs of all subcircuits have been determined, the GAM of the whole component is obtained by properly connecting the common ports. A very efficient method to determine the resulting GAM has been introduced in [6]: by using this algorithm the GAM of the whole component is obtained still in the same form of a pole expansion (5).

B. Calculation of the Dispersion Diagram

The dispersion diagram of SISW structures can be obtained along the lines of [7]. The method is based on the solution of an eigenvalue problem, which is obtained by imposing the periodicity of the field on the ports of the unit cell of the structure. The eigenvalues of the problem give the propagation constants of the SISW modes, and the corresponding eigenvectors are the values of $V_i^{(p)}$ defined in (1), representing the weight coefficients of the SISW electric fields on the ports in terms of TE_{p0} modes of the rectangular waveguide.

If it is not possible to identify a unit cell where the external ports are defined on homogeneous sections (i.e., they do not intersect any air holes), the method presented in the previous subsection cannot be used for calculating the GAM of the unit cell. In this case, however, the BI–RME method can still be used for the calculation of the dispersion diagram, by using a different approach. This approach, derived from a well–known measurement technique, consists in the analysis of two SISW sections with different length (*e.g.*, three and five cells), connected to the exterior through rectangular waveguides. The propagation constant is then derived from the difference of phase between the scattering parameters.

III. Numerical and Experimental Results

Two examples are reported in this section, to validate the proposed numerical method and to show the performance of SISW structures.

The first example refers to a rectangular waveguide, filled with a dielectric medium perforated with two holes per unit cell (Fig. 3*a*). The analysis of the unit cell was performed with our code, in order to calculate the GAM of the structure. Ten modes were considered in each waveguide port. Then, by using the Floquet theorem, the dispersion diagram of the first modes was determined. The propagation constant of the first two modes versus the frequency is reported in Fig. 3*b*, and compares very well with the results obtained by HFSS. This SISW operates in the X and Ku band, with the cutoff frequency of the fundamental mode at 6.85 GHz and the cutoff frequency of the second mode

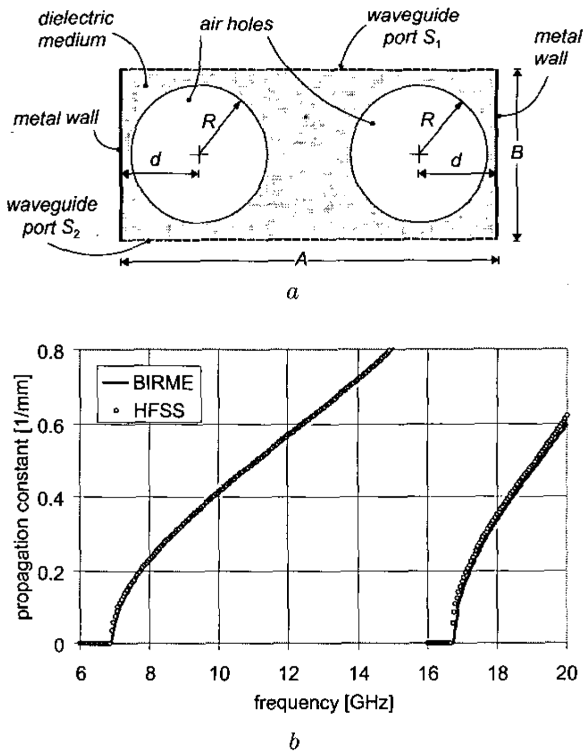

Fig. 3. SISW with two holes per unit cell: (*a*) cross–section of the unit cell. Dimensions in mm: $A = 8.2$, $B = 3.7$, $d = 1.7$, $R = 1.5$; dielectric constant $\epsilon_r = 10.2$; (*b*) dispersion diagram of the first two modes calculated by the BI–RME method and a commercial code (HFSS).

at 16.65 GHz.

The analysis of the unit cell also provides the weight coefficients of the SISW modes on the modes of the rectangular waveguide. The weight coefficients of the first SISW mode on the first three (odd) waveguide modes are reported in Fig. 4. They show that only the fundamental waveguide mode plays a significant role in the representation of the first SISW mode in the whole band. A limited contribution comes from TE_{30} mode, being all other modes practically negligible. It is also observed that, considering only these modes in the GAM representation of the unit cell, the dispersion diagram of the first two SISW modes does not change. The calculation of the dispersion diagram of this structure was also performed considering two structures with different length and the results are in good agreement with the one obtained by using the unit cell.

The second example refers to a SISW optimized for operating in both X and Ku band. The unit cell of this structure presents six holes with different size (Fig. 5*a*). Their location was chosen in such a way to maximize the air/dielectric ratio in the side regions of the waveg-

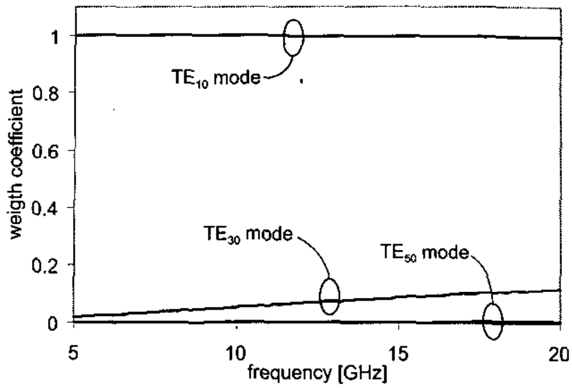

Fig. 4. SISW with two holes per unit cell: weigth coefficients of the fundamental modes on the waveguide modes versus frequency.

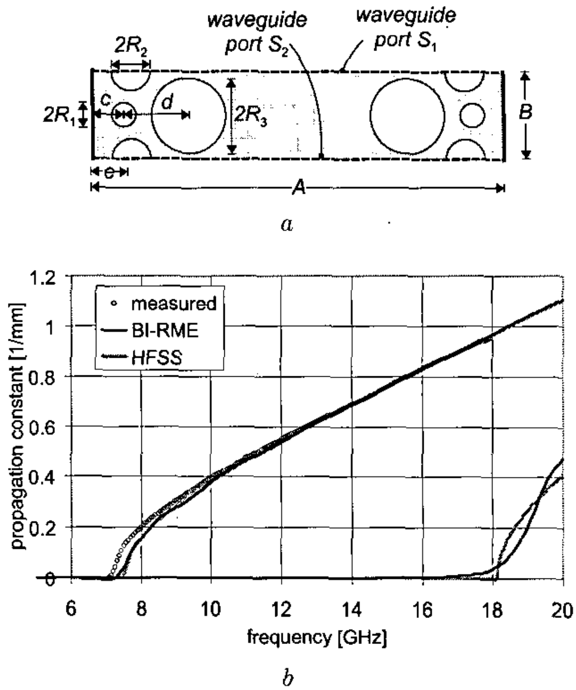

Fig. 5. SISW with optimized hole configuration: (a) cross-section of the unit cell. Dimensions in mm: $A = 7.4$, $B = 1.7$, $c = 0.7$, $d = 1.25$, $e = 0.8$, $R_1 = 0.25$, $R_2 = 0.40$, $R_3 = 0.75$; dielectric constant $\epsilon_r = 10.2$; (b) dispersion diagram of the first two modes calculated by the BI-RME method, compared with measurements and with HFSS.

uide (and therefore its bandwidth) and satisfying, at the same time, the fabrication constraint (minimum spacing between holes). As shown in Fig. 5a, this structure prevents us from using the BI-RME method for the analysis of the unit cell. Therefore, the dispersion diagram was obtained using the second approach described in Sect. II, from the comparison of the scattering parameters of two waveguide sections with different length.

The structure was fabricated, substituting the rectangular waveguide with a SIW structure, as described in [7]: the side walls of the rectangular waveguide were replaced by arrays of metallic holes. The dispersion diagram of the first two modes calculated by the BI-RME method is reported in Fig. 5b, and compared with the measured data (limited to the first mode) and the simulation by HFSS. The BI-RME analysis presents a good agreement both with the measurement and with HFSS.

IV. Conclusion

This paper presented a novel method for the analysis of Substrate Integrated Slab Waveguides, based on a rectangular waveguide filled with a periodically perforated dielectric medium. The characterization of the structure by the BI-RME method was outlined, along with two techniques for the calculation of the dispersion diagram of these integrated guides. An integrated structure, able to cover two bands (X and Ku), compact and easy to fabricate was presented. The examples demonstrated both the accuracy of the numerical method and the performance of these structures.

References

[1] D. Deslandes, M. Bozzi, P. Arcioni, and K. Wu, "Substrate Integrated Slab Waveguide (SISW) for Wideband Microwave Applications," submitted to *International Microwave Symposium 2003*.

[2] P. H. Vartanian, W. P. Ayres, and A. L. Helgesson, "Propagation in Dielectric Slab Loaded Rectangular Waveguide," *IRE Trans. Microwave Theory & Tech.*, pp. 215–222, April 1958.

[3] G. Conciauro, M. Guglielmi, and R. Sorrentino, *Advanced Modal Analysis*, John Wiley and Sons, 2000.

[4] G. Conciauro, P. Arcioni, M. Bressan, L. Perregrini, "Wideband Modeling of Arbitrarily Shaped H-Plane Waveguide Components by the 'Boundary Integral-Resonant Mode Expansion Method'," *IEEE Trans. Microwave Theory & Tech.*, Vol. MTT-44, No. 7, pp. 1057–1066, July 1996.

[5] P. Arcioni, M. Bressan, G. Conciauro, and L. Perregrini, "Generalized Y-Matrix of Arbitrary H-Plane Waveguide Junctions by the BI-RME Method," *International Microwave Symposium Digest (IMS1997)*, pp. 211–214, 1997.

[6] P. Arcioni and G. Conciauro, "Combination of Generalized Admittance Matrices in the Form of Pole Expansions," *IEEE Trans. Microwave Theory & Tech.*, Vol. MTT-47, No. 10, pp. 1990–1996, Oct. 1999.

[7] Y. Cassivi, L. Perregrini, P. Arcioni, M. Bressan, K. Wu, G. Conciauro, "Dispersion characteristics of substrate integrated rectangular waveguide," *IEEE Microwave & Wireless Components Letters*, Vol. 12, No. 9, pp. 333–335, Sept. 2002.